



10-4-11

RESPONSE OF CYLINDRICAL TANKS SUBJECTED TO LATERAL LOADS CORRELATION BETWEEN ANALYTICAL AND EXPERIMENTAL RESULTS

George C. MANOS¹ and Dimosthenis TALASLIDIS¹

¹ Department of Civil Engineering, Structural Engineering Division,
Aristotle University, Thessaloniki 54006, GREECE.

SUMMARY

Following the earthquake damage of cylindrical liquid storage tanks from past strong earthquakes, the earthquake response of these structures has attracted considerable attention. This paper examines the response of an "Aluminum Broad Tank" model subjected to static-tilt loading, as it was observed during an experimental study, which was also followed by a numerical investigation. In addition, the tank wall stability performance of this model as well as that of a number of other models during similar static tilt test conditions is also examined and discussed.

INTRODUCTION

This paper studies the behavior of metal cylindrical liquid storage tanks subjected to earthquake loading by examining the response of this type of structure when the horizontal inertia effects are approximated by a static "tilt test" type loading arrangement. This is achieved by tilting the base that supports the examined tank with respect to the horizontal plane. In this way the hydrostatic pressure acting on the tank wall becomes unsymmetrical thus resulting in a horizontal shear force and an overturning moment acting on the structure that approximates similar resultant forces generated by horizontal earthquake ground motion. Although the hydrostatic pressures in a "static tilt" test loading arrangement may differ in their distribution from the hydrodynamic pressures produced by horizontal earthquake ground motions, because of the similarity in the resultant forces acting on the structure it may be used as a substitute loading for studying the behavior of tanks subjected to earthquakes, especially for response mechanisms that develop in both the actual earthquake excitation as well as in the static tilt test loading arrangement. A major advantage of the static tilt test is that it can be performed more easily than a dynamic test and the response of the studied structure can be examined in detail under static loading conditions both experimentally and analytically. This "static tilt" test arrangement was used by Shih (ref. 2) together with small plastic models. Clough and Niwa (ref. 1) used a "static tilt" test arrangement in parallel with the shaking table earthquake loading to examine the behavior of a large "Berkeley Aluminum Tall Model Tank" whereas Manos and Clough (ref. 3) did the same but this time for a large "Berkeley Aluminum Broad Model Tank". Peek et.al. (ref. 8) used also a similar loading arrangement to examine small tank models made of plastic "Caltech. Mylar Tank Models"), whereas Sakai et.al.(ref. 11) similarly studied both small plastic tanks ("Kawasaki Mylar Tank Models") as well as one large

aluminum tank model ("Kawasaki Aluminum Model Tank"), the largest of all models studied so far under similar conditions (see also Table 1). A series of "static tilt" tests are under way at the Laboratory of Strength of Materials of the Department of Civil Engineering of Aristotle University of Thessaloniki, Greece, as part of a study on the behavior of liquid storage tanks to lateral loads (Photo 1).



Photo 1. Thessaloniki Tank Model

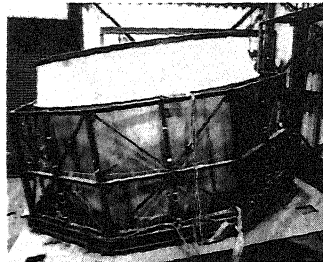


Photo 2. Berkeley Broad Tank Model

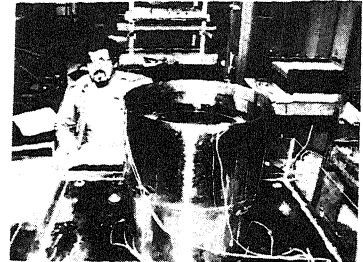


Photo 3. Thessaloniki Tank on Shaking Table

EXPERIMENTAL INVESTIGATION

The model tank studied by Manos and Clough (ref. 3) was a ground supported aluminum tank model 3.66m in diameter and 1.83m high; it was filled with water to a depth of 1.52m and it simulated an actual steel prototype tank three times larger (Photo 2). Details on the instrumentation and the experimental results are presented by Manos and Clough together with the relevant conclusions in a number of publications (refs. 3,5 and 6). Figures 1 and 2 depict the measured radial displacements at the top-rim and mid-height sections of the tank wall whereas figures 3 and 4 depict the uplift displacement and the "uplift penetration" at the tank bottom. In figures 5 and 6 the circumferential distribution of the axial and the shear membrane stress is plotted, respectively; this was measured at 16 locations at a horizontal tank wall section two inches from the bottom. All these measurements, plotted with crosses (+) with respect to the solid line representing the tank wall, were recorded when the tilting angle was kept constant and equal to 16 degrees and the tank bottom was free to uplift resting on the rigid foundation. All this plotted response is with respect to an initial reference condition when the tank is at zero tilt and full of water to a depth of 1.52m.

In the last part of the paper experimental results, obtained from a recent test, are utilised together with results from tests performed by other researchers. The studied tank, designated as "Thessaloniki Bronze A", was 0.50m in diameter and 0.60m high and it was filled with water at a depth of 0.50m (Photo 1). It was subjected to tilting of its base, when it was resting on a relatively stiff foundation made of plaster with the tank bottom free to uplift. The same tank was also subjected to earthquake excitations on the shaking table of the same laboratory (ref. 10 and Photo 3). Radial and uplift displacements were recorded at various points of the model together with strains at a limited number of points on the wall near the bottom of the tank. The formation of any instability on the tank wall was also recorded visually (Photo 4).

NUMERICAL INVESTIGATION

The "Berkeley Aluminum Broad Tank", which was briefly described above, was also studied analytically using the finite element method. As this investigation

is still under way only limited results will be presented herein. The behavior of this model was analysed for two different base conditions; first, with the tank base clamped at the supporting rigid platform and second with the bottom of the tank free to uplift from the rigid base. The third base condition, which was studied experimentally by placing a rubber mat as foundation material, is not yet considered in the analysis. For all analysed cases the hydrostatic load was initially applied, representing the pressures for zero tilt angle, and this loading condition was solved first. Then, the hydrostatic load resulting from the pressures at 16 degrees tilt was next applied and a solution for this loading case was obtained. The difference in the displacement and stress results between the 16 and zero degrees tilt solutions represent the values that are comparable with the corresponding experimental measurements and are plotted in figures 4 to 8. By ignoring the initial irregularities of the tank wall and taking into account the distribution of the hydrostatic pressures resulting from tilting, the structure can be analysed assuming symmetry with respect to the axis of tilt (N-S, Fig. 7); in this way only one half of the structure was discretised. Another simplification was to omit the inner part of the bottom plate in the discretisation. In this artificially produced boundary, at a radius $R=0.711m$, all displacements were constrained to be zero. The remaining outer circle of the bottom plate (from $R=0.711m$ to $R=1.88m$) was discretised by 96 quadrilateral flat shell elements. The same number and type of elements was also used to discretise the tank wall. Finer mesh was used at areas of the structure whereby large gradients of displacements and stresses were expected to develop, as shown by the experimental measurements. Finally, 14 beam elements were used in order to model the wind girder that was present at the top-rim section of the aluminum "broad tank" model. More details on the features of the used discretisation are given in reference 9.

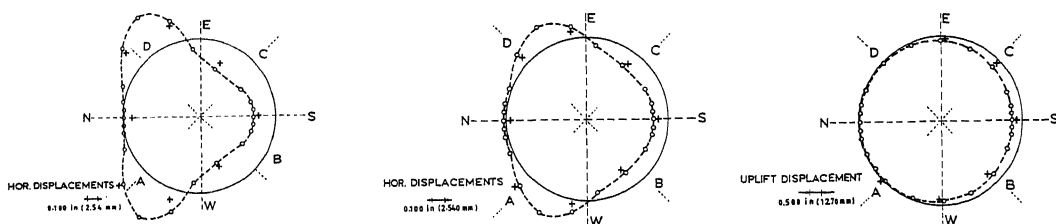


Fig. 1. Horiz. Displacements Top-Rim Section Fig. 2. Horiz. Displacements Mid-Height Section Fig. 3. Uplift Displac. Bottom Plate

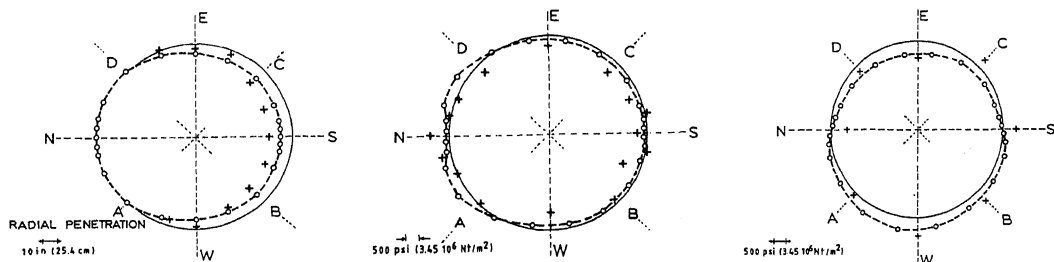


Fig. 4. Uplift Penetration Bottom Plate Fig. 5. Axial Stresses 2" from Bottom Fig. 6. Shear Stresses 2" from Bottom

NUMERICAL TREATMENT OF THE UPLIFT BEHAVIOR

When the structure is clamped at the bottom it can be assumed that the used clamping devices prohibit any uplifting of the tank bottom from taking place. In this case all three displacements at the shell to bottom plate intersection were constrained to zero and the structure was analysed by the direct stiffness method using the described finite element discretisation. However, in order to analyse the case whereby the tank is experiencing uplift during the tilt loading arrangement, as evidenced by the experimental investigation, the changing boundary condition at the contact area between the tank bottom plate and the foundation during the loading process must also be considered. In order to treat this type of nonlinearity the finite element method was used together with a numerical iterative procedure. The support of the tank bottom to the foundation was approximated by elastic springs located at the nodes of the described finite element discretisation (Fig. 7); these springs were assumed that they could transmit load only to one direction (compression) whereas they could not withstand any tension thus allowing the bottom plate uplift to occur. In this case of unilateral boundary conditions, such as at the contact between bottom plate and foundation during uplift, the iterative procedure that was used in conjunction with the finite element method is based on theorems proved for quadratic optimization problems whereby the unilateral problem is replaced equivalently by a number of classical bilateral problems performing iterations in such a manner that convergence to the solution of the unilateral problem is assured. This procedure is presented in reference 4 by Talaslidis and Panagiotopoulos and it will not be repeated here. Figure 7 depicts the used discretisation, which also includes the supporting unilateral elastic springs between the bottom plate and the foundation.

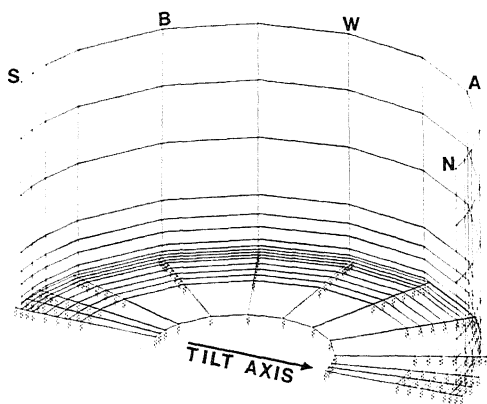


Figure 7. Used Discretisation

Some of the numerical results obtained from the unanchored tank analysed in this way for a 16 degrees tilt angle are presented in figures 1 to 6, plotted as circles, together with the corresponding experimental measurements. Figures 1 and 2 depict the top-rim and mid-height magnified displacements as they actually occur; the solid line represents the undeformed tank wall. Relatively good agreement can be seen between numerical and experimental results. Figure 3 depicts the circumferential distribution of the base uplift, which is plotted inwards from the solid-line circle representing the joint between the tank wall and the annular plate. It can also be seen from this figure that relatively good agreement can be observed between the F.E.M. results and the measured uplift in this case.

As already mentioned, the contact area between the bottom plate and the rigid foundation was recorded during the experiments by measuring the base uplift "radial penetration" towards the center of the tank. The circumferential distribution of this parameter is plotted in figure 4 at various points around the wall-to-plate joint for both the analysis and the experiment. It can be seen that the numerical solution underestimates this penetration near the North-South tank diameter (tilt-axis), whereas the opposite is true near the East-West diameter. Finally, figures 5 and 6 depict the circumferential distribution of the axial (vertical) and shear membrane stresses at a horizontal section two inches from the tank bottom where the stress response was measured during the experiment at 16 points around the tank-circumference, indicated by the crosses in this plot. The corresponding numerical results were found by averaging the stress values at the centroid of two successive tank wall rectangular elements, with

regard to the used discretisation along the wall height. For each position the centroids of these elements are located in the used discretisation at the same circumferential angle, with a distance of one inch and three inches from the tank bottom, respectively. As can be seen from the plotted distribution of the stress response, noticeable discrepancies can be observed between the measured and the calculated stresses. For the shear membrane stress there is reasonable agreement between measured and predicted response in the maximum values as well as in the overall stress distribution pattern. However, although there is relatively reasonable agreement in the maximum compressive axial membrane stress values, the observed in this case stress distribution includes regions of stress concentration near the tilt axis (N) that differ from the corresponding stress concentration regions predicted by the F.E.M. solution.

TANK-WALL STABILITY DURING TILT-TEST CONDITIONS

Table 1 presents a summary of tilt tests that were performed with metal as well as with plastic unanchored tank models, which experienced uplift during the test sequence. The maximum reported tilt angle is listed in column (1) of this table for every case together with corresponding maximum measured response parameters and the observed tank wall behavior (columns 1,2,3 and 9). The same table also lists in column 4 the corresponding theoretical buckling stress for each model, whereas column 6 lists the maximum resisting overturning moment (OM_{res}), which was found following the procedure of reference 7. However, because this procedure was proposed for actual earthquake conditions it is modified here with respect to only one parameter; that is the maximum compressive axial membrane stress (σ_{max}) at the tank wall was taken equal to 50% of the theoretical buckling stress instead of 75% that was used in reference 7. This reduction represents an arbitrary approximation in order to account for the difference between the static nature of the tilt-test loading and the dynamic nature of the pressures induced on the flexible tank wall by the earthquake excitation. Finally, columns 7 and 8 of Table 1 list the corresponding ratios between maximum observed over predicted stress and overturning moment response. These ratios together with the observed tank wall stability performance for each test are additional verifications of the used empirical procedure (ref.7) which is proposed for predicting tank wall instability for uplifting tanks, when subjected to actual earthquake excitations. As can be seen in this table, for all cases whereby no shell instability was observed the ratio of predicted over observed overturning moment is well above 1. For most of the cases whereby a collapse of the tank model was observed the value of this ratio is well below 1. For the appearance of the first buckling the value of this ratio is either smaller or larger than 1, but the difference from 1 is not much in most cases with the exception of the last case ("Caltech. Mylar H=5, reference 8).

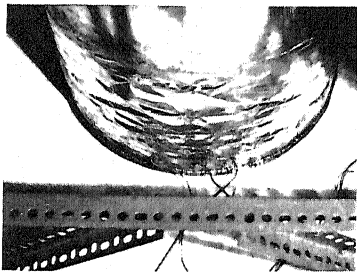


Photo 4. Thessaloniki Tank Collapse Mode.

CONCLUSIONS

1. The comparison between numerical and experimental results for one static tilt test of "Berkeley Aluminum Broad Tank", supported on a rigid foundation and free to uplift, demonstrated that the displacement response can be reasonably predicted in this way whereas for the stress response discrepancies were observed between experimental and numerical results.
2. The utilisation of the static-tilt test tank wall stability observations and the subsequent comparison with predictions made by the empirical procedure proposed by the first author is additional positive evidence of its validity.

REFERENCES

- 1) Clough, R.W. Niwa, A., and Clough, D.P. "Experimental Seismic Study of Cylindrical Tanks", Journal of the Structural Division, ASCE, Vol. 105, ST12, pp. 2565-2590, December, 1979.
- 2) Shih, C.F. "Failure of Liquid Storage Tanks Due to Earthquake Excitation ", Ph.D. Thesis submitted to California Institute of Technology, May, 1981.
- 3) Manos, G.C., and Clough, R.W. "Further Study of the Earthquake Response of a Broad Cylindrical Liquid-Storage Tank Model", EERC Report No. 82/07, UCB, California, 1982.
- 4) Talaslidis, D., and Panagiotopoulos, P., "A Linear Finite Element Approach to the Solution of the Variational Inequalities Arising in Contact Problems of Structural Dynamics", Int. Journal Num. Meth. in Eng., Vol. 18, pp. 1505-1520, 1982.
- 5) Manos, G.C. and Clough, R.W. "Dynamic Response Correlation of Cylindrical Tanks", Proc. Symposium in Lifeline Earthquake Engineering, pp. 190-221, ASCE Convention, San Fransisco, California, 1984.
- 6) Manos, G.C. "Dynamic Response of a Broad Storage Tank Model under a vareity of Simulated Earthquake Motions", Proc. 3rd U.S. National Conference on Earthquake Engineering, Vol. III, pp. 2131-2142, Charleston, S.C., 1986.
- 7) Manos, G.C. "Earthquake Tank Wall Stability of Unanchored Tanks", ASCE, Journal, Structural Division, Vol. 112, No. 8, pp. 1863-1880, 1986.
- 8) Peek, R., Jennings, P.C. and Babcock, C.D., "The Preuplift Method for Anchoring Fluid Storage Tanks", 3rd U.S. National Conference on Earthquake Engineering, Vol. III, pp. 2155-2164, 1986.
- 9) Manos, G.C. and Talaslidis, D., "Experimental and Numerical Study of Unanchored Cylindrical Tanks Subjected to Lateral Loads", Proceedings 3rd Int. Conf. on Comput. Meth. and Exper. Measur., pp. 487-495, Greece, 1986.
- 10) Manos, G.C., "Anchored Tank Fundamental Period Approximation Employing Non-Uniform Shell Thickness", Bulletin ERS, Inst. Ind. Science, University of Tokyo, No. 20, pp. 81-84, March, 1987.
- 11) Sakai, F., et.al. "Experimental Study on Up-lift Behavior of Large-sized Cylindrical Liquid Storage Tanks", Proc., PVP Conference, ASME, June 1987, San Diego, California.

Table 1. Summary of Static Tilt tests

Tank Description	Tilt Angle (deg)	Maximum Observed		Theoret. Buckling Stress (Mpa)	Found. Flex. Coeff.	Predic. Overt. Moment (Nt m)	Predic. / Observed		Observed Tank-Wall Stability
		Axial Stress (Mpa)	Overt. Moment (Nt m)				Axial Stress Ratio	Overt. Moment Ratio	
	(1)	(2)	(3)	(4)	(5)	(6)	(7)	(8)	(9)
Berkeley Aluminum Broad Rigid (ref. 3)	16.0	5.146	33968	46.368	1.0	169816	4.505	5.00	Not Buckled
Berkeley Aluminum Broad Flex. (ref. 3)	16.0	4.815	33968	46.368	1.5	254724	4.808	7.47	Not Buckled
Berkeley Aluminum Tall Rigid (ref. 1)	8.5	28.627	49935	80.776	1.0	120759	1.412	2.42	Not Buckled
Kawasaki Aluminum Rigid (ref 11)	12.3	13.727	1621889	43.506	1.0	2805395	1.587	1.73	Not Buckled
Thessaloniki Bronze A, Rigid	12.0 17.0	4.532 ---	50.17 70.77	17.983 17.983	1.0 1.0	38.88 38.88	1.984 ---	0.78 0.55	Before First Buckle Collapsed
Kawasaki Mylar A (ref. 11)	20.8	---	78.04	4.532	1.0 1.25	49.31 61.63	---	0.63 0.79	Collapsed
Kawasaki Mylar B (ref. 11)	17.8	---	434.28	2.725	1.0 1.25	308.54 385.49	---	0.71 0.89	Collapsed
Caltech. Mylar H=10, (ref. 8)	3.0	---	0.209	2.476	1.0	0.231	---	1.10	First Buckle
Caltech. Mylar H=5, (ref. 8)	8.8	---	0.153	2.476	1.0	0.262	---	1.62	First Buckle